Journal of
Experimental
Botany
www.jxb.oxfordjournals.org

RESEARCH PAPER

Anatomical basis of variation in mesophyll resistance in eastern Australian sclerophylls: news of a long and winding path

Tiina Tosens[1,2,*], Ülo Niinemets[2], Mark Westoby[1] and Ian J. Wright[1]

[1] Department of Biological Sciences, Macquarie University, New South Wales 2109, Australia
[2] Institute of Agricultural and Environmental Sciences, Estonian University of Life Sciences, Kreutzwaldi 64, Tartu 51014, Estonia

*To whom correspondence should be addressed. E-mail: Tiina.Tosens@emu.ee

Abstract

In sclerophylls, photosynthesis is particularly strongly limited by mesophyll diffusion resistance from substomatal cavities to chloroplasts (r_m), but the controls on diffusion limits by integral leaf variables such as leaf thickness, density, and dry mass per unit area and by the individual steps along the diffusion pathway are imperfectly understood. To gain insight into the determinants of r_m in leaves with varying structure, the full CO_2 physical diffusion pathway was analysed in 32 Australian species sampled from sites contrasting in soil nutrients and rainfall, and having leaf structures from mesophytic to strongly sclerophyllous. r_m was estimated based on combined measurements of gas exchange and chlorophyll fluorescence. In addition, r_m was modelled on the basis of detailed anatomical measurements to separate the importance of different serial resistances affecting CO_2 diffusion into chloroplasts. The strongest sources of variation in r_m were S_c/S, the exposed surface area of chloroplasts per unit leaf area, and mesophyll cell wall thickness, t_{cw}. The strong correlation of r_m with t_{cw} could not be explained by cell wall thickness alone, and most likely arose from a further effect of cell wall porosity. The CO_2 drawdown from intercellular spaces to chloroplasts was positively correlated with t_{cw}, suggesting enhanced diffusional limitations in leaves with thicker cell walls. Leaf thickness and density were poorly correlated with S_c/S, indicating that widely varying combinations of leaf anatomical traits occur at given values of leaf integrated traits, and suggesting that detailed anatomical studies are needed to predict r_m for any given species.

Key words: Anatomical model, cell wall thickness, diffusion limitations of photosynthesis, interspecific variability, leaf economics spectrum, mesophyll diffusion.

Introduction

Leaf photosynthesis is determined by biochemical limitations (photosynthetic capacity) and diffusion limitations, including stomatal resistance and CO_2 diffusion resistance from substomatal cavities to the carboxylating enzyme, Rubisco, in the chloroplasts (so-called 'mesophyll diffusion resistance') (Flexas *et al.*, 2008, 2012; Terashima *et al.*, 2006, 2011). The concept of mesophyll resistance (r_m, see Table 1 for symbol definitions) can be described as follows. After entering the leaf through the stomata, CO_2 faces a relatively long and tortuous pathway through gas and liquid phases before it finally reaches the carboxylating

enzyme Rubisco. First, CO_2 must diffuse through the intercellular airspaces to a mesophyll cell surfaces adjacent to the airspace to enable free access for the CO_2. Gas diffusion in the liquid phase is slow, therefore CO_2 is most likely to enter the cell where the chloroplast directly abuts the cell wall (Terashima *et al.*, 2006, 2011). This process could be greatly enhanced if the cell walls were fully lined with chloroplasts, a condition that in practice is rare (Terashima *et al.*, 2006). CO_2 dissolves in the water-filled pores of the cell wall (Evans *et al.*, 2009) and diffuses across the cell wall. Diffusion across cell walls is slow if

Table 1. Symbols and units used

Variable	Definition	Unit
A	Net assimilation rate	$\mu mol\ m^{-2}\ s^{-1}$
C_c	CO_2 concentration in chloroplasts	$\mu mol\ mol^{-1}$
C_i	CO_2 concentration in intercellular airspace	$\mu mol\ mol^{-1}$
$C_i–C_c$	CO_2 drawdown from intercellular airspace to chloroplasts	$\mu mol\ mol^{-1}$
D_a	Diffusion coefficient for CO_2 in the gas phase	$m^2\ s^{-1}$
d_{leaf}	Leaf density	$g\ cm^{-3}$
D_w	Aqueous phase diffusion coefficient for CO_2	$m^2\ s^{-1}$
f_{ias}	Fraction of mesophyll occupied by intercellular airspace	Dimensionless
f_{pal}	Fraction of mesophyll cell volume comprised of palisade tissue	Dimensionless
$H/(RT_k)$	Henry´s law constant	Dimensionless
ΔL_{ias}	Effective diffusion path length in the gas-phase	m
L_{mes}	Total length of chloroplasts facing the intercellular airspace	m
L_{mes}	Total length of mesophyll cells facing the intercellular airspace	m
p_i	Effective porosity in the given part of the diffusion pathway	Dimensionless
Q	Incident quantum flux density	$\mu mol\ m^{-2}\ s^{-1}$
R	Gas constant	$Pa\ m^3\ K^{-1}\ mol^{-1}$
$r'm$	Mesophyll resistance of exposed chloroplast surface area per unit of leaf area	$m^2_{chlor}\ s\ mol^{-1}$
$r_{cellular}$	Cellular resistance, sum of r_{cw}, r_{pl}, r_{cyt}, r_{env}, and r_{str}	$s\ m^{-1}$
R_d	Dark respiration rate	$\mu mol\ m^{-2}\ s^{-1}$
r_{cw}	Cell wall resistance	$s\ m^{-1}$
r_{pl}	Plasma membrane resistance	$s\ m^{-1}$
r_{cyt}	Cytoplasm resistance	$s\ m^{-1}$
r_{env}	Chloroplast envelope resistance	$s\ m^{-1}$
r_{str}	Stroma resistance	$s\ m^{-1}$
r_{gas}	Gas phase resistance	$s\ m^{-1}$
r_{liq}	Liquid phase resistance	$s\ m^{-1}$
r_m	Mesophyll diffusion resistance	$m^2\ s\ mol^{-1}$
S_c/S	Chloroplast surface area exposed to intercellular airspace per unit of leaf area	$m^2\ m^{-2}$
s_{mes}	Cross-sectional surface area of mesophyll cells in micrograph	m^2
s_{pal}	Cross-sectional area of palisade mesophyll cells in micrograph	m^2
s_s	Cross-sectional area of mesophyll cells in micrograph	m^2
$S_{c,pal}/S$	S_c/S for palisade mesophyll	%
$S_{c,spon}/S$	S_c/S for spongy mesophyll	%
S_c/S_{mes}	Ratio of exposed chloroplast to mesophyll surface areas	Dimensionless
S_{mes}/S	Surface area of mesophyll cells exposed to airspace per unit of leaf area	$m^2\ m^{-2}$
t_{chlor}	Chloroplast thickness	μm
t_{cw}	Cell wall thickness	μm
T_k	Absolute temperature	K
t_{leaf}	Leaf thickness	mm
t_{mes}	Mesophyll thickness	mm
W	Width of the section measured	m
γ	Curvature correction factor	Dimensionless
$\gamma_{f,i}$	Proportional reduction of diffusion conductance in the cytosol and in the stroma compared with free diffusion in water	Dimensionless
ς	Diffusion path tortuosity	$m\ m^{-1}$
Γ^*	Hypothetical CO_2 compensation point without R_d	$\mu mol\ mol^{-1}$
Φ_{PSII}	Effective quantum yield of PSII	Dimensionless
ξ	Leaf absorptance	Dimensionless
ε	Fraction of electrons absorbed by PSII	Dimensionless

the walls are lignified and porosity is low, and/or if the walls are thick. Diffusion through the cytoplasmic layer between the cell wall and the chloroplast is fast if chloroplasts are closely appressed to the cell walls. Chloroplasts are relatively thick organelles, and diffusion through the chloroplast could potentially be one of the most limiting steps in CO_2 physical diffusion, unless most Rubisco were located close to the chloroplast inner

envelope membrane (Tosens *et al.*, 2012) or carbonic anhydrase operated close to Rubisco to enhance the apparent diffusion gradient (Terashima *et al.*, 2011).

All of these anatomical features pose partial resistances for CO_2 diffusion and contribute to the total mesophyll resistance. Slower CO_2 diffusion through the mesophyll causes larger CO_2 concentration gradients between the stroma and intercellular

airspaces, C_i–C_c (Niinemets and Sack, 2006; Warren, 2008; Niinemets *et al*., 2009*c*). Ignoring the fact that CO_2 concentration in chloroplasts (C_c) is often lower than the CO_2 concentration in substomatal cavities (C_i) leads to the underestimation of Rubisco-related photosynthetic parameters (Flexas *et al*., 2006*a*., 2007; Niinemets *et al*., 2009*a*) and biased respiration rate calculations (Ayub *et al*., 2011). Although this is now quite widely recognized, r_m is still generally ignored in large-scale carbon gain models due to our lack of knowledge about why it varies among species, and how best to model it (Warren, 2008; Niinemets *et al*., 2009*c*).

The gas-phase pathway is longer than the liquid-phase pathway but gas diffusion in the liquid phase is approximately 10 000-fold slower (Evans *et al*., 1994; Terashima *et al*., 2006). Gas-phase resistance is thought to be negligible in thin and porous mesophytic leaves (Terashima *et al*., 2006; Flexas *et al*., 2008). Further, it has been demonstrated that gas-phase resistance is lower than liquid-phase resistance in thick, densely-packed, hypostomatous sclerophyll leaves (Syvertsen *et al*., 1995; Piel *et al*., 2002). Therefore, it is largely agreed that the main limitations to CO_2 diffusion are in the liquid phase (Flexas *et al*., 2009; Terashima *et al*., 2006, 2011).

Only a limited number of studies have analysed r_m together with its direct structural correlates. In some studies (Loreto *et al*., 1992; Evans *et al*., 1994; Tosens *et al*., 2012), a strong negative relationship has been reported between r_m and the area of exposed chloroplast surface per unit of leaf surface area, S_c/S. However, in others, no relationship has been found between S_c/S and r_m (Kogami *et al*., 2001; Gorton *et al*., 2003). On the other hand, a strong positive relationship between cell wall thickness and r_m was reported by Hassiotou *et al*. (2010). Overall, the information about the aqueous-phase structural determinants of r_m is conflicting and largely missing (Flexas *et al*., 2008; Warren, 2008; Evans *et al*., 2009).

CO_2 diffusion across the mesophyll is particularly slow in structurally robust leaves, (Niinemets and Sack, 2006; Flexas *et al*., 2008; Niinemets *et al*., 2009*c*, 2011). Because of stronger mesophyll diffusion limitations, evergreen sclerophylls are less sensitive to variations in stomatal openness (Niinemets *et al*., 2011); therefore, r_m is an important factor affecting photosynthetic performance in those species (Warren and Adams, 2006; Niinemets and Sack, 2006). Strong positive correlations between CO_2 drawdown from substomatal cavities to chloroplasts (a measure of CO_2 diffusion limitation of photosynthesis) and leaf dry mass per unit area (LMA; a measure of leaf robustness) have been observed across the species worldwide (Niinemets *et al*., 2009*c*), including Australian sclerophylls (Niinemets *et al*., 2009*b*). In the current study, 32 Australian sclerophyll species were examined for anatomical restrictions to CO_2 diffusion. The central aim was to identify and quantify the main sources of variation in r_m in these species. The data were fitted to the diffusion model of Niinemets and Reichstein (2003*a*) to unravel the importance of various components of the CO_2 diffusion pathway from substomatal cavities to Rubisco in the chloroplasts. In addition, the influence of anatomical traits on r_m was quantified and C_i–C_c calculated from gas exchange measurements. Finally, we turn to the question of what features of leaves are conducive to high chloroplast exposed areas per unit surface area, this being

one of the two leading dimensions determining total mesophyll resistance. All acronyms used are defined in Table 1.

Materials and methods

Study sites and species

The field measurements were conducted in April 2006 as described in detail by Niinemets *et al*. (2009*b*). In brief, plant material for gas-exchange measurements and foliage chemical and structural analyses was sampled from healthy individuals of 32 Australian evergreen tree and shrub species. Sampling was primarily spread across four sites (HRHN, high rain, high nutrients; HRLN, high rain, low nutrients; LRHN, low rain, high nutrients; LRLN, low rain, low nutrients) selected in native forests and shrublands near Sydney, Australia (see Table 2 for species sampled at each site). The open- or closed-forest vegetation supported at each site is characterized by broad-leaved canopy trees (e.g. *Eucalyptus* spp., *Corymbia* spp., *Syncarpia glomulifera*), with a mix of broad-leaved, needle-leaved, and microphyllous species in the understorey. To get a broader range of leaf structures and photosynthetic capacities, additional samples for five species were taken from Macquarie University campus (MQ; Table 2). In all cases, mature individuals were used. All species, except *Acacia* spp., possessed true mature leaves. *Acacia* spp. possessed foliage phyllodes that are analogues of broad leaves. It is noted that important structural changes occur in leaves upon transition from the juvenile to the mature leaf form and upon replacement of juvenile foliage by phyllodes in *Acacia* species (Ullmann, 1989; Groom *et al*., 1997). Ontogenetic modifications in leaf form are also associated with alterations in leaf anatomy and mesophyll diffusion conductance (Mullin *et al*., 2009; Steppe *et al*., 2011). Such modifications constitute a potentially highly important source of species differentiation among different habitats during ontogeny, but such modifications were not studied here. Further details about sites, species, and sampling procedures can be found in Niinemets *et al*. (2009*b*).

Measurement protocols and determination of diffusion limits of photosynthesis

The detailed measurement protocol is reported in Niinemets *et al*. (2009*b*). In brief, terminal branches were cut under water in the field in morning hours during high air humidity, transported to the laboratory and stabilized under dim light of 50–100 µmol m^{-2} s^{-1} and at 22 °C for 1–2 d to ensure the full hydration of branches and stable stomatal conductance during gas exchange measurements. Preliminary experiments demonstrated that while the stomatal conductance was relatively high immediately after branch sampling, the stomatal conductance rapidly declined during photosynthesis measurements conducted right after branch sampling. By contrast, stomatal conductances were high and stable in preconditioned branches (Niinemets *et al*., 2005, 2009*b*).

CO_2 response curves of net assimilation and steady-state fluorescence were measured with a Li-6400 gas-exchange system equipped with a Li-6400-40 Leaf Chamber Fluorometer (Li-Cor, Inc., Lincoln, Nebraska, USA) at a leaf temperature of 25 °C and incident quantum flux density of 1000 µmol m^{-2} s^{-1}. All gas-exchange rates were corrected for water vapour and CO_2 diffusion according to Rodeghiero *et al*. (2007). Gas-exchange rates and chlorophyll fluorescence measurements were used to determine the mesophyll diffusion resistance (r_m; see Table 1 for the units and abbreviations used in this study) from substomatal cavities to chloroplasts according to the variable electron transport rate method of Harley *et al*. (1992):

$$r_m = C_i / A - \frac{\Gamma^* f \quad A\varepsilon\Phi_{PSII}\zeta Q + 8(A + R_d)}{\varepsilon\Phi_{PSII}\zeta Q - 4(A + R_d)} \qquad (1)$$

where A is the net assimilation rate, C_i is the CO_2 concentration in substomatal cavities, R_d is the rate of non-photorespiratory

Table 2. Average thickness of key anatomical traits determining cellular resistance for the 32 study species from five sites

Species	Site[a]	Component thickness (µm)		
		Chloroplasts	Cell walls	Cytosol
Acacia longifolia	MQ	1.50	0.300	0.138
Acacia myrtifolia	HRLN	1.50	0.262	0.103
Acacia suaveolens	HRLN	1.65	0.367	0.162
Angophora hispida	HRLN	1.46	0.378	0.152
Astrotrichia floccosa	HRHN	1.71	0.330	0.132
Banksia aemula	LRLN	1.29	0.350	0.143
Banksia integrifolia	MQ	1.88	0.300	0.140
Banksia marginata	HRLN	1.30	0.388	0.111
Banksia oblongifolia	HRLN	1.36	0.380	0.141
Banksia robur	MQ	1.80	0.283	0.141
Banksia serrata	MQ	1.60	0.388	0.140
Banksia serrata	HRLN	1.57	0.380	0.142
Banksia spinulosa	LRHN	1.41	0.380	0.142
Eriostemon australasius	HRLN	1.59	0.321	0.142
Eucalyptus fibrosa	LRHN	1.28	0.374	0.143
Eucalyptus haemastoma	LRHN	1.67	0.367	0.090
Eucalyptus sclerophylla	LRLN	1.28	0.420	0.129
Eucalyptus umbra	HRHN	1.43	0.410	0.130
Grevillea speciosa	HRLN	1.74	0.335	0.142
Hakea dactyloides	HRLN	1.32	0.408	0.140
Lambertia formosa	HRHN	1.73	0.300	0.140
Lambertia formosa	HRLN	1.58	0.395	0.150
Macadamia ternifolia	MQ	1.34	0.342	0.141
Macrozamia communis	HRHN	1.88	0.263	0.150
Macrozamia spiralis	LRHN	1.44	0.373	0.140
Notolea longifolia	HRHN	1.37	0.365	0.130
Persoonia lanceolata	HRLN	1.59	0.325	0.142
Persoonia laurina	LRLN	1.61	0.310	0.141
Persoonia laurina	LRHN	1.44	0.331	0.143
Persoonia levis	HRLN	1.66	0.300	0.142
Pittosporum undulatum	MQ	1.83	0.281	0.145
Polyscias sambucifolia	MQ	1.80	0.252	0.150
Syncarpia glomulifera	HRHN	1.87	0.290	0.140
Synoum glandulosum	HRHN	1.57	0.278	0.135
Xylomelum pyriforme	HRHN	1.56	0.340	0.139

a HRHN, higher rain, high nutrients; MQ, Macquarie University campus (also higher rain); HRLN, higher rain, low nutrients; LRHN, lower rain, high nutrients; LRLN, lower rain, low nutrients. High rainfall sites experience *c*. 1220 mm annual rainfall, low rainfall sites *c*. 800 mm (climate data from the Australian Bureau of Meteorology; further site details given by Niinemets *et al.*, 2009*b*).

respiration, Γ^* is the hypothetical CO_2 compensation point without R_d (42.9 µmol mol^{-1} at 25 °C) derived *in vivo* by Bernacchi *et al.* (2001). Q is the incident quantum flux density, Φ_{PSII} is the effective quantum yield of PSII, $\xi\cdot$ is the leaf absorptance determined separately by an integrated sphere (Niinemets *et al.*, 2009*b*), and ε is the fraction of electrons absorbed by PSII (taken as 0.5). The values of r_m were calculated for measurements of net assimilation rate over the C_i range of 150–350 µmol mol^{-1}, and the average value of r_m was determined for each leaf. Over this range, r_m estimations are almost independent of C_i (Flexas *et al.*, 2007).

Light and electron microscopy

Small leaf discs around 5.8 mm in diameter were removed from the leaves used for gas exchange measurements. Care was taken to avoid big leaf vessels. The leaf sections were infiltrated in a syringe with the fixative 2% glutaric aldehyde in 0.1 M cacodylate buffer (pH=7.4), and

post-fixed in 2% buffered osmium tetroxide at 22 °C for 2 h. The samples were further dehydrated for 0.5 h at 22 °C in an ethanol series and embedded in a LR White resin for an hour at 22 °C. Leaf sections of 1 µm for light microscopy, and ultrathin sections of 70 nm for transmission electron microscopy (TEM) were made with Reichert–Jung ultra-cut ultra microtome (Leica, Vienna, Austria). The light microscope sections were stained with Toluidine blue and viewed in brightfield at magnifications of ×10 and ×40 by an Olympus BX 50 compound microscope, and photographed with a Scion CFW-1310 colour digital camera. The ultrathin sections were stained with lead citrate and viewed at magnifications of ×1800–×14 000 by a Philips CM10 TEM microscope (Philips, Eindhoven, The Netherlands), and photographed with an Olympus-SIS Megaview digital camera.

Mesophyll surface area exposed to intercellular airspace per unit leaf area, S_{mes}/S, and S_c/S (chloroplast area facing the outer surface of exposed mesophyll cell walls per unit leaf area) were calculated from light and TEM micrographs (magnification ×4200) following the method of Syvertsen *et al.* (1995). Thus, S_{mes}/S, is given as:

$$S_{mes} / S = \frac{L_{mes}}{W} \gamma \text{,} \tag{2}$$

where W is the width of the section measured, L_{mes} is the total length of mesophyll cells facing the intercellular airspace, and γ is the curvature correction factor that depends on the shape of the cells (Evans *et al.*, 1994) and was obtained as a weighted average for palisade and spongy mesophyll. Analogously, S_c/S, was calculated as:

$$S_c/S = \frac{L_c}{L_{mes}} S_{mes} / S \text{,} \tag{3}$$

where L_c is the total length of chloroplast surface area facing the intercellular airspace in the section.

The fraction of intercellular airspace (f_{ias}) was determined as:

$$f_{ias} = 1 - \frac{\sum s_s}{t_{mes} W} \tag{4}$$

where t_{mes} is the mesophyll thickness between the two epidermal layers and Σs_s is the sum of the cross-sectional areas of mesophyll cells.

The fraction of mesophyll cell volume comprised of palisade tissue (f_{pal}) was determined as:

$$f_{pal} = \frac{s_{pal}}{s_{mes}} \tag{5}$$

where s_{pal} is the cross-sectional area of cell surfaces that is palisade and s_{mes} is the cross sectional surface area of mesophyll cells.

Cell wall thickness (t_{cw}), cytoplasm thickness (t_{cyt}), and chloroplast thickness (t_{chlor}) were directly measured from TEM micrographs at a magnification of ×14 000. For a given section, all characteristics were determined at least in three different fields of view, and at least three different sections were analysed.

A model for calculation of internal mesophyll diffusion resistance

Values of S_c/S were used to calculate the mesophyll diffusion resistance of exposed chloroplast surface area r'_m ($r_m S_c/S$) as is common in studies of mesophyll diffusion limitations of photosynthesis (Evans *et al.*, 2009; Terashima *et al.*, 2006, 2011). r'_m is an appropriate variable in the correlative relationships with individual components of the diffusion pathway. A quantitative one-dimensional within-leaf gas diffusion model was applied to gain an insight into the partial determinants of mesophyll diffusion resistance from substomatal cavities to chloroplasts (for the full details of the model see Niinemets and Reichstein, 2003*a*; Tosens *et al.*, 2012). In the model, the total mesophyll resistance (gas-phase

equivalent), r_m, is separated between gas-phase resistance from substomatal cavities to the outer surface of cell walls (r_{gas}) and gas-phase equivalent liquid-phase resistance from the outer surface of cell walls to the chloroplasts (r_{liq}) (Evans et al., 1994; Niinemets and Reichstein, 2003a, b):

$$r_m = r_{gas} + \frac{r_{liq}RT_k}{H} \qquad (6)$$

where H is the Henry's law constant (Pa m^3 mol^{-1}), R is the gas constant (Pa m^3 K^{-1} mol^{-1}) and T_k is the absolute temperature (K). $H/(RT_k)$ is the dimensionless form of Henry's law constant (gas/liquid phase partition coefficient) that is needed to convert, r_{liq}, a resistance in the liquid phase to gas-phase equivalent resistance. At 25 °C used in our study for gas-exchange measurements, $H/(RT_k)$ for CO_2 is 1.2 (Dodds et al., 1956; Umbreit et al., 1972).

Gas-phase diffusion depends on the fraction of mesophyll volume occupied by intercellular airspace (f_{ias}, m^3 m^{-3}) and the effective diffusion path length in the gas-phase (ΔL_{ias}) (Syvertsen et al., 1995) as:

$$r_{gas} = \frac{\Delta L_{ias}\varsigma}{D_a f_{ias}} \qquad (7)$$

where ς is the diffusion path tortuosity (m m^{-1}) and D_a (m^2 s^{-1}) is the diffusion coefficient for CO_2 in the gas-phase (1.51×10^{-5} m^2 s^{-1} at 25 °C). ΔL_{ias} was approximated by half of the mesophyll thickness (Niinemets and Reichstein, 2003a). An estimate of ς can be obtained from paradermal and transverse leaf sections (Terashima et al., 1995), but its estimation is laborious and relatively imprecise due to varying geometry of leaf cells, making it difficult to discern the sites where air passages are blocked. In addition, ς may also vary with environmental conditions. A fixed value of ς of 1.57 m m^{-1} was used, as previously employed by Syvertsen et al. (1995) and Niinemets and Reichstein (2003a).

A total liquid phase resistance is given as the sum of the serial resistances:

$$r_{liq} = \left(r_{cw} + r_{pl} + r_{cyt} + r_{env} + r_{str} \right)/\left(S_c / S \right) \qquad (8)$$

where the partial resistances are: r_{cw} for cell wall, r_{pl} for plasmalemma, r_{cyt} for cytosol, r_{env} for the chloroplast envelope, and r_{str} for the chloroplast stroma. $r_{cellular}$ was defined further as the sum of $r_{cw}+r_{pl}+r_{cyt}+r_{env}+r_{str}$. Liquid phase resistance r_{liq} is lower if there is a broad pathway into mesophyll cell walls facing the chloroplasts (S_c/S), but higher if $r_{cellular}$ is high along a unit cross-section of that pathway. Accordingly, the contributions of pathway breadth S_c/S relative to $r_{cellular}$ were visualized by plotting $\log_{10}[(S_c/S)^{-1}]$ against $\log_{10}r_{cellular}$.

The cell wall, cytosol, and stroma resistances (r_i) are given by a general equation (Nobel, 1991):

$$r_i = \frac{\Delta L_i}{\gamma_{f,i} D_w p_i} \qquad (9)$$

where ΔL_i (m) is the diffusion path length and p_i (m^3 m^{-3}) is the effective porosity in the given part of the diffusion pathway, D_w is the aqueous phase diffusion coefficient for CO_2 (1.790×10^{-9} m^2 s^{-1} at 25 °C) and the dimensionless factor $\gamma_{f,i}$ accounts for the decrease of diffusion conductance in the cytosol and in the stroma compared with free diffusion in water (Weisiger, 1998). The values of $\gamma_{f,i}$ used were 1 for cell walls and 0.294 for the cytosol and stroma (Niinemets and Reichstein, 2003a). The diffusion pathlength was taken as equal to the cell wall thickness for r_{cw}, the average distance between the chloroplasts and cell wall for r_{cyt}, and half of the chloroplast thickness for r_{str} (Tosens et al., 2012). Although carbonic anhydrase could potentially affect r_{str} in non-steady-state conditions (Evans et al., 2009; Terashima et al., 2011), the evidence of the involvement of carbonic anhydrase in determining r_{str} is currently equivocal and was not considered in the current study to avoid additional assumptions [see Discussion and Tosens et al. (2012) for further discussion].

Effective porosity, p_i, was taken as 1 for r_{cyt} and r_{str}. Initially, a constant value of 0.05 was applied for the porosity of cell walls (Terashima et al., 2006). However, as there is evidence that effective porosity decreases with increasing thickness of the cell walls (Evans et al., 2009), a least squared iterative analysis was used instead, varying the p_i of the cell wall to get the best fit (highest r^2) between the measured and modelled r_m values. Best fit was obtained by varying p_i linearly from 0.095 at the lowest cell wall thickness of 0.252 μm to 0.040 at the maximum cell wall thickness of 0.420 μm. This method is referred to as the variable p_i approach.

CO_2 diffusion resistance through the plasma membrane (r_{pl}) and chloroplast envelope membranes and (r_{env}) cannot be estimated from micrographs. In addition, the CO_2 diffusion rate through membranes can be modified by aquaporins (Flexas et al., 2006b, 2012; Hanba et al., 2004). However, it has been suggested that CO_2 permeability through lipid bilayers is high, on the order of 0.03 m s^{-1}, and therefore aquaporins have only a minor impact on CO_2 permeability (Missner et al., 2008). By contrast, it was suggested by Boron et al. (2011) that membrane permeability can be two orders of magnitude less and aquaporins play a key role in membrane permeability. As suggested in the review of Evans et al. (2009), aquaporins could limit 30% of the lipid-phase diffusion resistance at most. Membrane permeability can be estimated from CO_2 lipid-phase solubility using structure–function relationships as suggested by Niinemets and Reichstein (2003a), but information of the lipid-phase solubility of CO_2 is limited. Due to incomplete information about CO_2 diffusion through biological membranes, a constant value of 0.0035 m s^{-1} for both r_{pl} and r_{env} was used in the present study, as had been successfully employed by Evans et al. (1994) and Tosens et al. (2012).

Results

Performance of the anatomical model of mesophyll diffusion resistance

The species-mean estimates of r_m calculated from anatomical measurements were tightly correlated with the estimates obtained from coupled gas-exchange/fluorescence measurements (Fig. 1, $r^2=0.84$, $P<0.0001$). This indicates that equations 6–9 provide a reasonable assessment of relative contributions of different leaf anatomical features to mesophyll resistance. The estimates made from anatomy tended to overestimate mesophyll resistance in low-resistance species and underestimate it in high-resistance species. The average (±SE) discrepancy between modeled and measured r_m was 15.6±0.03%.

Estimated liquid-phase resistance was consistently larger than gas-phase resistance, and varied more widely (Fig. 2). Most values of r_{liq} fell in the range of 250–600 s m^{-1} compared with 40–180 s m^{-1} for r_{gas}. Consequently, differences in r_m between species arose mainly from variations of the components of r_{liq}. Plotting $\log_{10}[(S_c/S)^{-1}]$ against $\log_{10}r_{cellular}$ to separate the contributions of the components of r_{liq} demonstrated that the variation in $(S_c/S)^{-1}$ spanned about 0.5 $\log_{10}$ units (i.e. c. 3-fold; Fig. 3a). The sum of resistances along a unit cross-section of the pathway as estimated by equations 6–9 varied rather narrowly, by about 0.1 $\log_{10}$ units (Fig. 3a). Chloroplasts represent potentially the longest diffusion path in the liquid phase (Table 2). Nevertheless, the largest contribution to $r_{cellular}$ resulted from cell walls, being more than 50% in all species (Table 3). These values were estimated assuming a constant cell wall porosity of
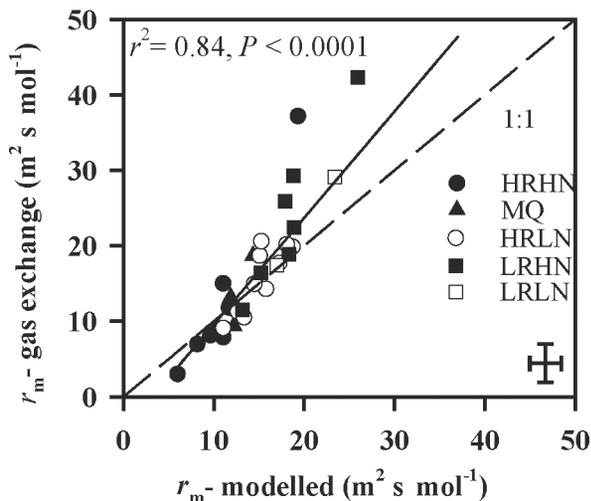
Fig. 1. Correlation between mesophyll diffusion resistance determined from combined gas-exchange and chlorophyll fluorescence measurements (equation 1, r_m, gas exchange) and mesophyll resistance calculated from anatomical data (equations 6–9, r_m, modelled). Data were fitted by linear regression. The error bars in the lower right corner indicate the maximum size of standard errors across species. HRHN, higher rain, high nutrients; MQ, Macquarie University campus; HRLN, higher rain, low nutrients; LRHN, lower rain, high nutrients; LRLN, lower rain, low nutrients. See Table 2 for studied species and site information.
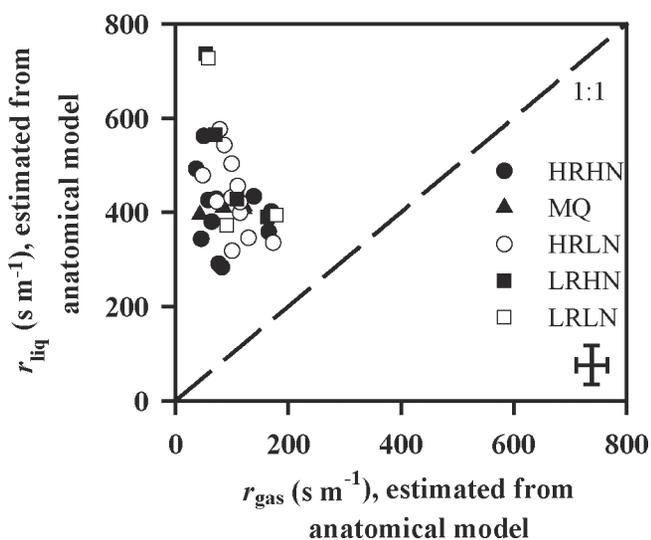
Fig. 2. Relationship between the CO_2 diffusion resistance in liquid (r_{liq}) and gas phase (r_{gas}). r_{liq} is the sum of partial cellular resistances in cell wall (r_{cw}), plasmalemma (r_{pl}), cytosol between cell wall and chloroplast (r_{cyt}), chloroplast envelope (r_{env}), and chloroplast stroma (r_{str}) multiplied by the inverse of chloroplast exposed to total leaf surface area ratio (S_c/S)$^{-1}$: $(r_{cw}+r_{pl}+r_{cyt}+r_{env}+r_{str})/(S_c/S)$. In the r_{liq} calculations, we assumed a mesophyll cell wall porosity of 0.05 for all species. Representation of symbols and error bars as in Fig. 1.
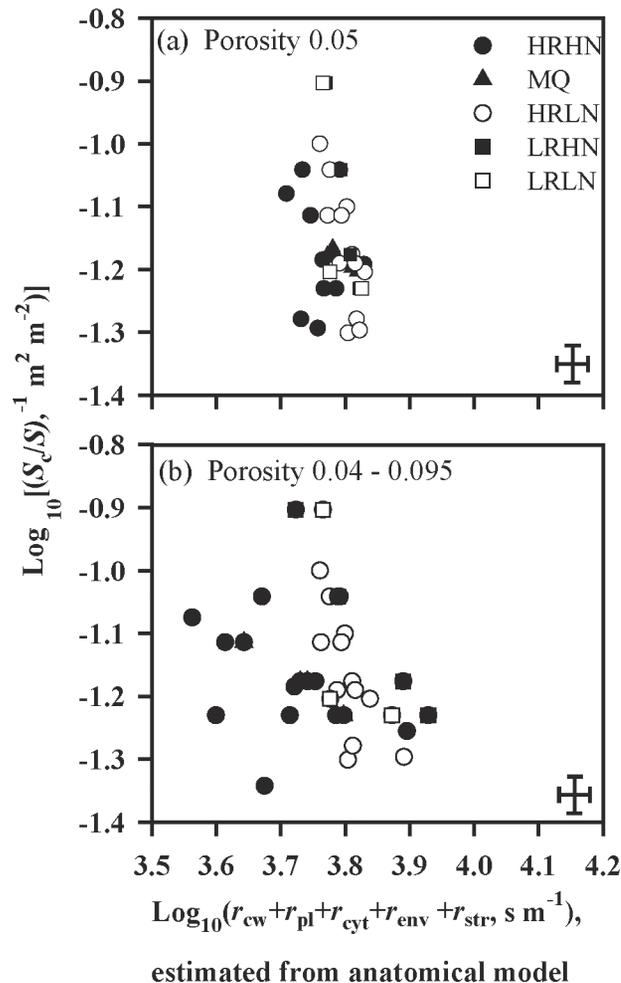
Fig. 3. Relationship between the inverse of chloroplast surface area exposed to intercellular airspace per unit leaf area $(S_c/S)^{-1}$, and the sum of individual cellular resistances $[(r_{cw}+r_{pl}+r_{cyt}+r_{env}+r_{str})]$. Both axes are log-transformed. Log (liquid-phase resistance) is the sum of these two log-components, $Log[(S_c/S)^{-1}]$ and $Log(r_{cw}+r_{pl}+r_{cyt}+r_{env}+r_{str})$ and increases towards the upper right corner. The sum of serial liquid-phase resistances was calculated assuming a constant mesophyll cell wall porosity of 0.05 for all species (a), or assuming variable porosity of mesophyll cell walls, with porosity ranging from 0.040 to 0.095, decreasing with increasing depth of cell wall (b). A constant value of 0.0035 m s^{-1} was assigned to both r_{pl} and r_{env}. Symbols and error bars as in Fig. 1.

0.05 in all species. However, when the porosity of cell walls was assumed to decrease with increasing the thickness of cell walls as described in the Materials and methods, $r_{cellular}$ was predicted to be at least as important as S_c/S in determining the variation in r_m across the species (Fig. 3b).

Mesophyll cell wall as an important contributor to mesophyll resistance

Mesophyll cell wall thickness was a strong predictor of interspecific variation in mesophyll resistance per unit of exposed chloroplast surface (r'_m, Fig. 4a). By contrast, variation in r'_m cal-

Table 3. Contribution of different components of cellular resistance to the total cellular resistance, estimated from the anatomical model for the 32 study species from five sites*1A constant mesophyll cell wall porosity of 0.05 was assumed for all species.

Species	Site[a]	Contribution to total cellular resistance (%)			
		Stroma	Cell walls	Cytosol	Membranes[b]
Acacia longifolia	HRHN	30.7	55.5	4.3	9.2
Acacia myrtifolia	HRLN	26.2	59.5	5.0	9.2
Acacia suaveolens	HRLN	24.0	62.6	4.7	8.7
Angophora hispida	HRLN	21.8	66.3	2.9	9.0
Astrotrichia floccosa	HRHN	27.8	57.2	3.8	11.2
Banksia aemula	LRLN	20.5	65.4	4.5	9.6
Banksia integrifolia	MQ	29.9	56.1	4.5	9.6
Banksia marginata	HRLN	19.5	68.2	3.3	9.0
Banksia oblongifolia	HRLN	20.3	66.6	4.2	9.0
Banksia robur	MQ	30.3	55.1	4.7	10.0
Banksia serrata	MQ	22.7	64.8	4.0	8.7
Banksia serrata	HRLN	22.7	64.5	4.1	8.7
Banksia spinulosa	LRHN	20.8	66.1	4.2	8.9
Eriostemon australasius	HRLN	25.4	60.4	4.5	9.6
Eucalyptus fibrosa	LRHN	18.0	69.0	4.1	8.6
Eucalyptus haemastoma	LRHN	29.9	55.9	3.3	10.9
Eucalyptus sclerophylla	LRLN	18.1	69.9	3.4	8.6
Eucalyptus umbra	HRHN	20.1	67.8	3.7	8.5
Grevillea speciosa	HRLN	20.5	60.0	4.3	9.2
Hakea dactyloides	HRLN	18.9	68.5	4.0	8.6
Lambertia formosa	HRHN	28.1	57.5	4.6	9.8
Lambertia formosa	HRLN	22.2	65.1	4.2	8.5
Macadamia ternifolia	MQ	21.4	64.4	4.5	9.7
Macrozamia communis	HRHN	32.0	52.6	5.1	10.3
Macrozamia spiralis	LRHN	19.6	67.0	4.3	9.2
Notolea longifolia	HRHN	21.0	65.8	4.0	9.2
Persoonia lanceolata	HRLN	25.2	60.7	4.5	9.6
Persoonia laurina	LRLN	26.3	59.3	4.6	9.8
Persoonia laurina	LRHN	23.2	62.6	4.6	9.7
Persoonia levis	HRLN	27.3	58.1	4.7	9.9
Pittosporum undulatum	MQ	30.4	54.8	4.8	10.0
Polyscias sambucifolia	MQ	31.7	52.4	5.3	10.6
Syncarpia glomulifera	HRHN	30.3	55.3	4.5	9.8
Synoum glandulosum	HRHN	27.5	57.2	4.7	10.6
Xylomelum pyriforme	HRHN	24.2	62.1	4.3	9.4

a Site codes as in Table 2.
b Membrane contribution is determined by the permeabilities of plasmalemma and chloroplast envelope membranes. These permeabilities were fixed at a constant value of 0.0035 m s^{-1} for all species. However, the contribution of membrane permeabilities to total cellular resistance varies due to the variation in numerical values for the other components of the diffusion pathway.

culated from anatomy (Fig. 4b) was only about as large as expected from the direct influence of cell wall thickness on resistance. Mesophyll cell wall porosity was treated initially as a constant of 0.05 in these calculations. When the porosity was assumed to decrease with increasing cell wall thickness (as in Fig. 3b), the consequence of the assumption of variable porosity was that the wall resistance varied across species considerably more widely than wall thickness per se – approximately 5-fold more (Fig. 4a, 4c).

Comparing Fig. 3b with Fig. 3a, the species from the high-rain high-nutrient site tended to be separate from the other species, towards lower $r_{cellular}$. They tended to have distinctly thinner mesophyll cell walls (Table 4), and the implications of that difference for wall resistance were amplified when porosity was assumed to be higher in thin-walled species. Chloroplast thickness and t_{cw} tended to co-vary in such a way that species with thick cell walls tended to have thinner chloroplasts adjacent to them (Fig. 5).

Structural limitations to r_m measured in the field

As expected, given the above results from model predictions, variation in t_{cw} and S_c/S predicted a considerable portion of that in r_m measured via gas exchange (Fig. 6a, 6b). The estimated CO$_2$ concentration drawdown from the internal airspace into the chloroplast (C_i–C_c) was well correlated with mesophyll cell wall thickness (Fig. 6c) but unrelated to S_c/S (Fig. 6d).
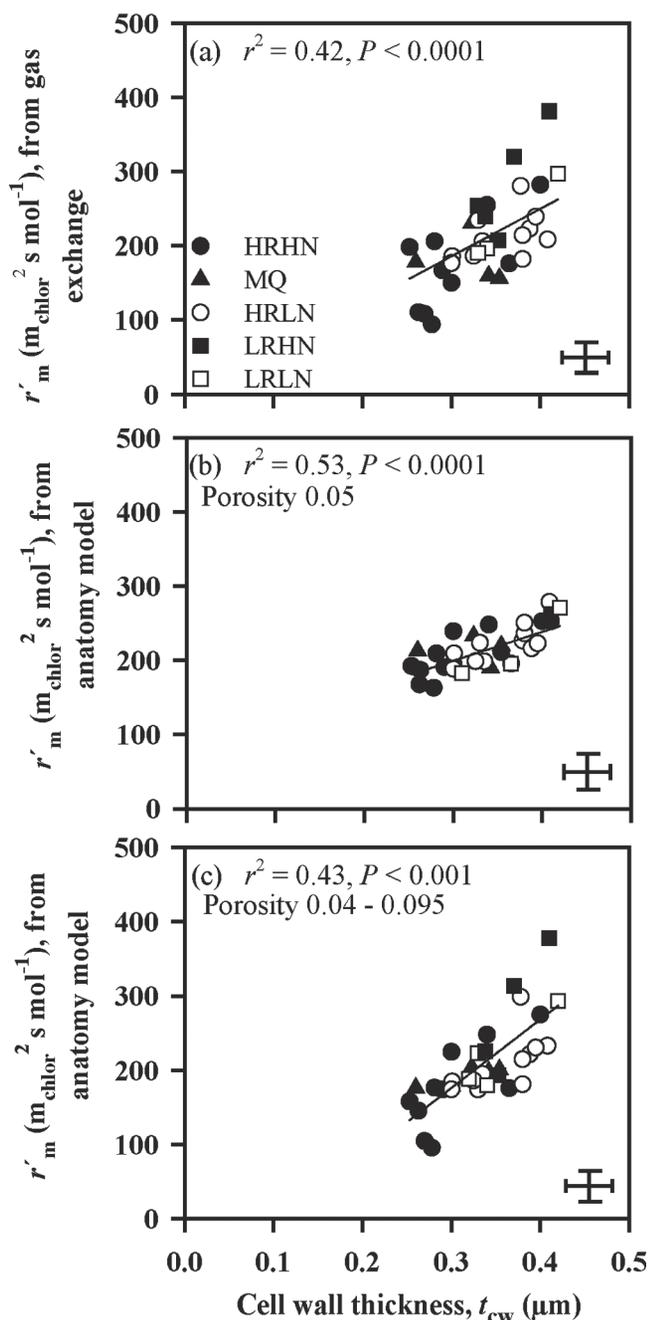
Fig. 4. Correlations between mesophyll resistance per unit exposed chloroplast surface area, r'_m and cell wall thickness (t_{cw}) for r'_m estimates derived from gas-exchange measurements (a) and modelled using anatomical data, either assuming a constant mesophyll cell wall porosity of 0.05 for all species (b) or varying the porosity (p_i) between 0.040 to 0.095 across species (c). In the latter case, the best fit was obtained by varying p_i linearly from 0.095 at the lowest cell wall thickness of 0.252 µm to 0.040 at the maximum cell wall thickness of 0.420 µm. Representation of symbols and error bars as in Fig. 1.

How Australian sclerophylls increase S_c/S

Finally, we turn to the anatomical features which lead to a highly exposed chloroplast area per unit surface area of the leaf
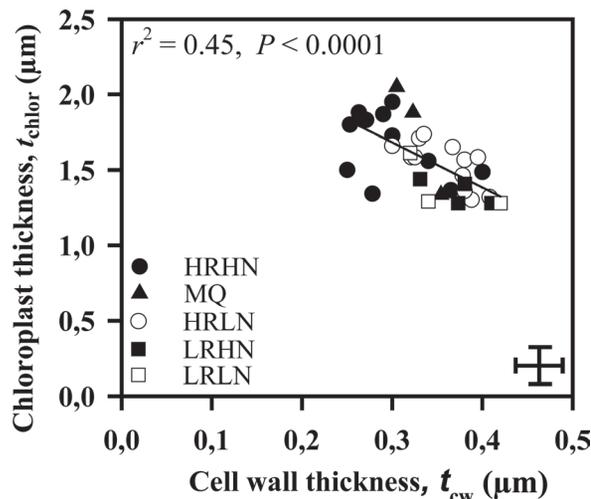
Fig. 5. The relationship between cell wall thickness, t_{cw}, and chloroplast thickness, t_{chlor} across the species. Data were fitted by linear regression. Symbols and error bars as in Fig. 1.

Table 4. Average (±SE) cell wall thickness (t_{cw}) and chloroplast surface area exposed to intercellular airspace per unit leaf area (S_c/S) in four contrasting environments
Means with the same letter are not significantly different (P >0.05). Only the species sampled from natural sites were included. The low rain, low nutrient site was not included in the statistical analysis due to limited sample size.

Site	t_{cw} (µm)	S_c/S (m² m⁻²)
High rain, high nutrient	0.322±0.030 a	15.3±1.0 a
High rain, low nutrient	0.356±0.012 b	13.4±1.0 a
Low rain, high nutrient	0.365±0.034 b	15.0±1.3 a
Low rain, low nutrient	0.360±0.033	13.7±1.1

(this being one of the two leading influences on total mesophyll resistance). S_c/S did not increase with the depth of the leaf lamina nor with the depth of mesophyll (see Supplementary Fig. S1a, b at *JXB* online). S_c/S and f_{ias} were negatively correlated (Fig. 7a).

The most important source of variation across species with regard to the exposed mesophyll cell surface, and hence in the exposed chloroplast surface, proved to be the fraction of mesophyll contributed by the palisade tissue (Fig. 7b). There seemed to be several factors contributing to this. First, although two-dimensional sections often give the impression that the palisade mesophyll is closely packed, in fact, many of its cell surfaces are adjacent to airspaces. Second, the proportion of cell surface occupied by exposed chloroplasts tended to be greater in palisade than in spongy tissue (data not shown). Third, the elongated shape of palisade cells means that they have more cell surface per volume than do spongy mesophyll cells. Fourth, palisade cells were quite small in many of the species studied here, which also increases the amount of cell surface per volume occupied. These tendencies are shown in Fig. 8a–d (transverse anatomical sections from selected species). Further, *c*. 50–90% of S_c/S was controlled by palisade compared with spongy mesophyll
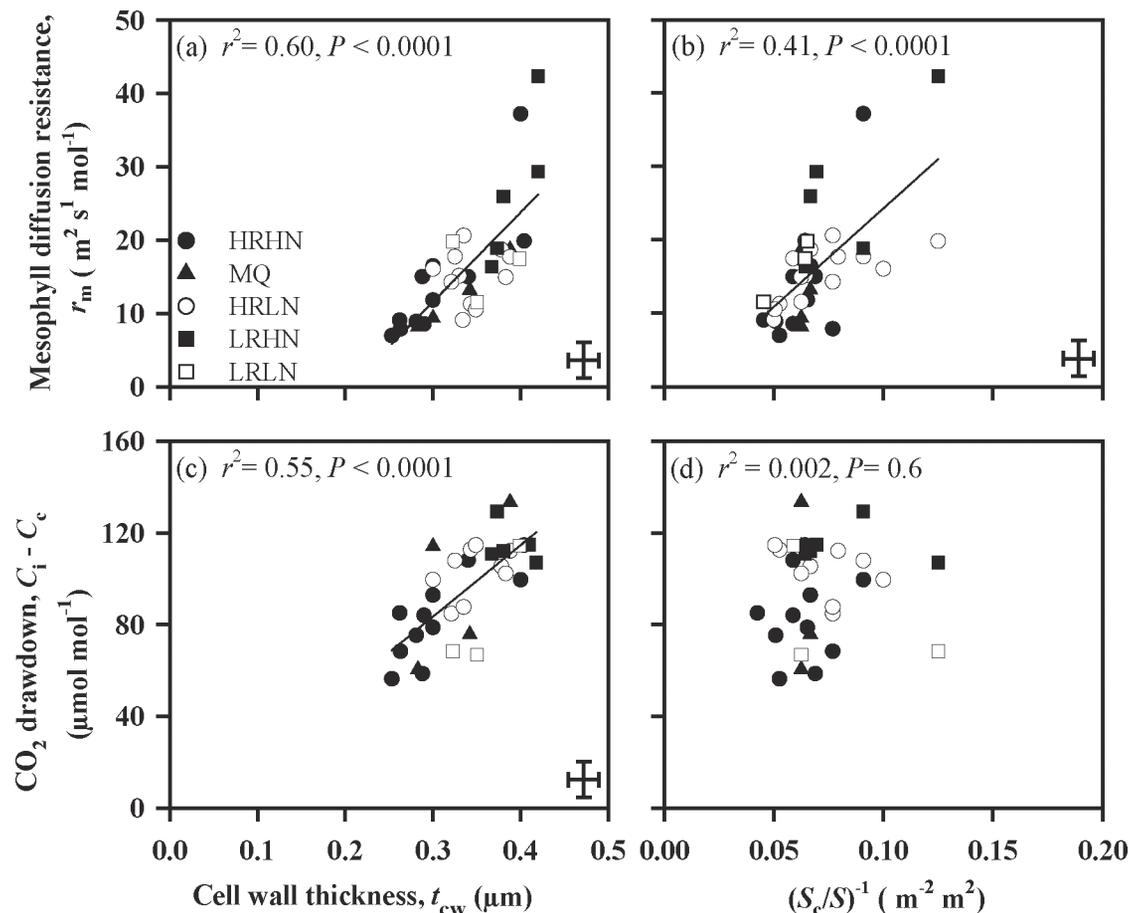
Fig. 6. Mesophyll resistance (r_m, (a, b) and CO_2 drawdown from intercellular airspace to chloroplasts (C_i–C_c, (c, d)) in relation to (a, c) mesophyll cell wall thickness, t_{cw}, and (b, d) chloroplast surface area exposed to intercellular airspace per unit leaf area (S_c/S). The data were fitted by linear regression. The symbols and error bars as in Fig. 1.
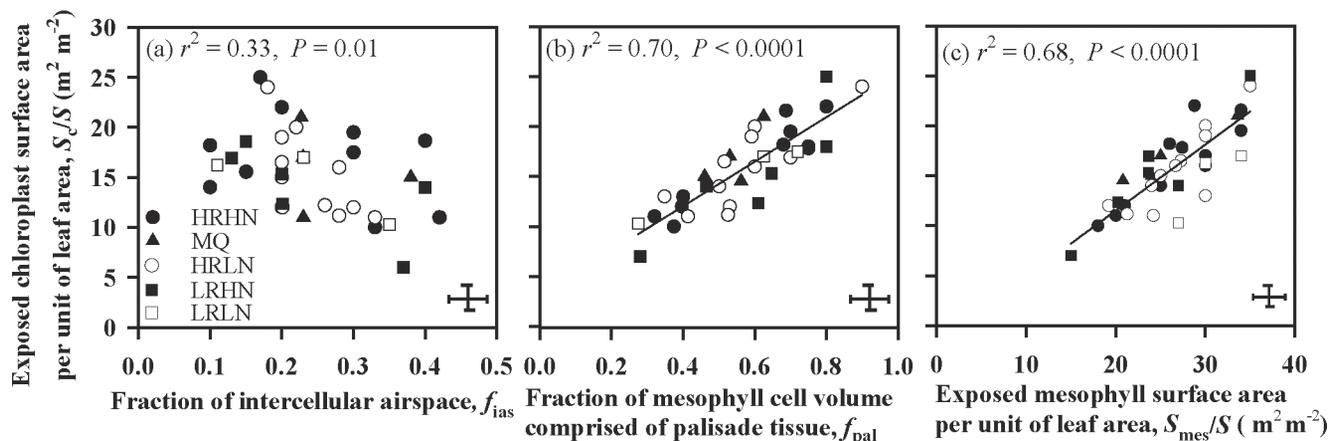
Fig. 7. Correlations of chloroplast surface area exposed to intercellular airspace per unit leaf area, S_c/S, (a) the fraction of mesophyll occupied by intercellular airspace, f_{ias}; (b) the fraction of mesophyll cell volume in palisade tissue, f_{pal}; and (c) mesophyll surface area exposed to intercellular airspace per unit leaf area, S_{mes}/S. The data were fitted by linear regressions. Data presentation and error bars as in Fig. 1.

among the study species (see Supplementary Table S1 at *JXB* online). As might be expected, the area of chloroplasts adjacent to airspaces was strongly correlated with the area of mesophyll cell surface adjacent to airspaces (Fig. 7c).

0.1mm
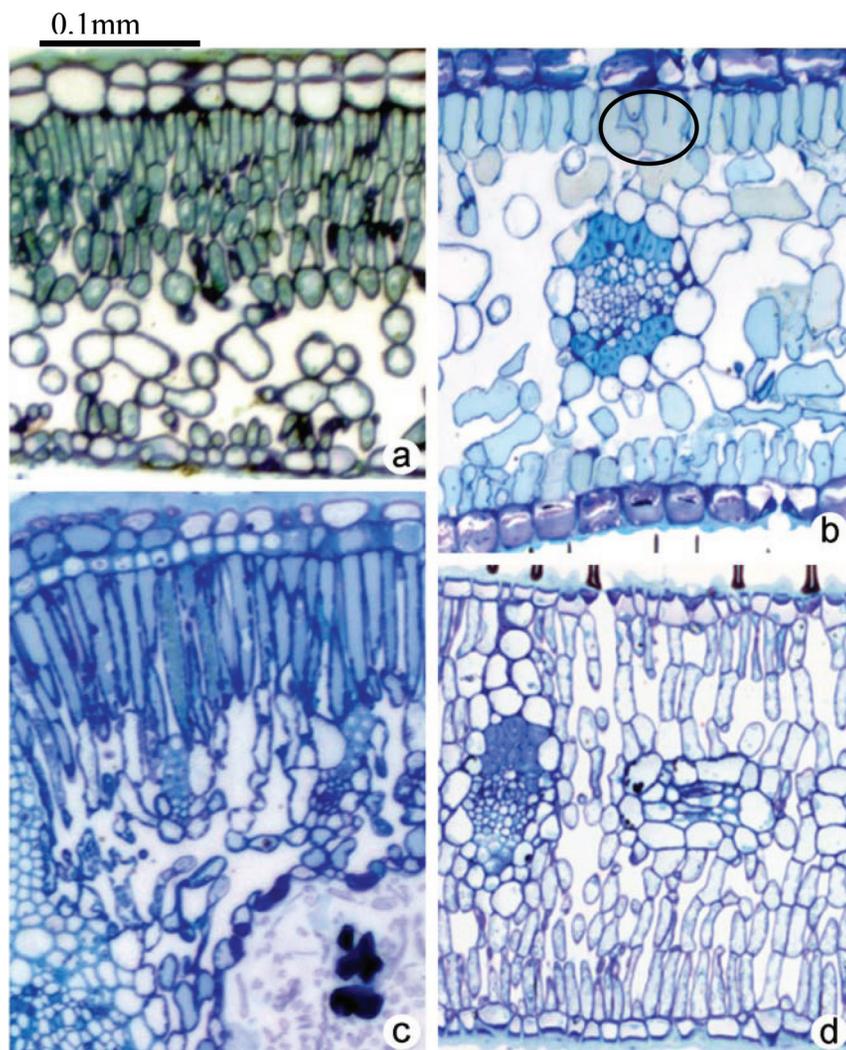
Fig. 8. Representative light micrographs of leaf transverse sections demonstrating the strategies in Australian species to reduce mesophyll resistance by increasing S_{mes}/S and S_c/S. (a) Stacked layers of small palisade cells in *Pittosporum undulatum*; (b) armed cells in *Persoonia lanceolata* leaf (inside the circle); (c) mesophyll cell elongation in *Banksia integrifolia*; and (d) multiple layers of palisade cells in the lower and upper leaf sides in *Eucalyptus haemastoma*. The sections were stained with Toluidine blue and the photos are taken at magnification of ×10.

Discussion

Diffusion model of mesophyll resistance

The correspondence between r_m data from the anatomical model and gas exchange measurements ($r^2 = 0.84$) can be considered good given that there are various uncertainties inherent to both measurement and modelling approaches (e.g. in gas exchange methods the assumptions concerning the fraction of light absorbed by PSII; Pons *et al.*, 2009). As argued above, in our view, the approach outlined in equations 6–9 allows for a trustworthy assessment of the relative contributions of different anatomical features to overall mesophyll resistance.

In our model, r_m is divided between two components, r_{gas} and r_{liq} (equation 6). r_{gas} increases with decreasing f_{ias} and increases with increasing leaf thickness, while r_{liq} increases with increasing the length of composite parts of the diffusion pathway and decreases with increasing S_c/S that determines the number of

parallel diffusion pathways into the cells (Terashima *et al.*, 2006). Because gas diffusion in the liquid phase is *c*. 10 000-fold slower than in the gas phase, the bulk of diffusional limitations is in the liquid phase (Syvertsen *et al.*, 1995; Piel *et al.*, 2002; Terashima *et al.*, 2006). Our study across Australian sclerophyll species supports the idea that r_{gas} is negligible compared with r_{liq}. Furthermore, r_{liq} varied more among species than did r_{gas} (Fig. 2). In the liquid phase, variation in $(S_c/S)^{-1}$ was greater than that in $r_{cellular}$, at least when cell wall porosity was assumed to be invariant (Fig. 3a).

It has been assumed that membranes of all species are similarly permeable to CO_2 and a constant permeability value suggested by Evans *et al.* (1994) was used. Under this assumption membranes contributed *c*. 8–11% of the total $r_{cellular}$ (Table 3). It has been suggested that CO_2 diffusion through membranes is regulated by aquaporins (Hanba *et al.*, 2004; Flexas *et al.*, 2006b; Terashima *et al.*, 2006, 2011). Primarily, aquaporins have

been associated with short-term fluctuations in r_m, for example, if plants are suddenly exposed to extreme drought (Terashima *et al.*, 2011), and it has been suggested that membrane permeability can be reduced by as much as two orders of magnitude (Boron *et al.*, 2011), while other studies suggest that the role of aquaporin is minor (Missner *et al.*, 2008; and the discussion in Flexas *et al.*, 2012). The debate over the role of aquaporins has clearly not yet settled, but, in our study, a satisfactory agreement between modelled and measured r_m was achieved by ignoring the possible interspecific variations in lipid phase resistance.

It was found that most chloroplasts were positioned close to cell walls, with only a very thin layer of cytosol in between. Cytoplasm thickness varied little among species and, on average, it accounted for *c*. 3–5% of the total liquid phase resistance (Table 3). Gillon and Yakir (2001) proposed that r_{str} is primarily controlled by carbonic anhydrase (CA) activity in the chloroplast. They suggested that CA activity is increasingly important to facilitate CO_2 diffusion in species with thick cell walls such as evergreen sclerophylls (Gillon and Yakir, 2001). At the normal cytosolic pH of 7.5, cytosolic CA should be sufficiently active to ensure the fast interconversion of CO_2 and bicarbonate. However, to date, there is little evidence that variation in cytosolic CA significantly influences r_m (Terashima *et al.*, 2006). In addition, the studies of Price *et al.* (1994) and Williams *et al.* (1996) with genetic transformants with low chloroplastic CA, indicated a minor effect of chloroplastic CA levels on photosynthetic performance. The results presented here suggested that r_{str} is controlled by the length of the physical CO_2 diffusion path in chloroplasts. This importance of chloroplast thickness is also indirectly supported by the fact that species with thicker mesophyll cell walls had thinner chloroplasts adjacent to these cell walls. Therefore, species with high cell wall resistance might be under particularly strong evolutionary selection to reduce r_{str} by minimizing the diffusion path length in chloroplasts.

Overall, the correspondence between measured and modelled estimates of diffusion resistance is striking (Fig. 1), and provides encouraging evidence that the principal processes governing interspecific variation in r_m were captured by the model. More complex 3D models have been developed (Aalto and Juurola, 2002; Tholen and Zhu, 2011), and such models probably have greater predictive capacity. However, parameterization of such models is currently highly time-consuming and the parameterizations are not general such that we feel that a simple 1D model as used here is more practical for interspecific comparisons where a large number of species needs to be examined.

Mesophyll cell wall as an important contributor to mesophyll resistance

The relationship between t_{cw} and mesophyll resistance calculated per unit of S_c/S was steeper than the observed variation in cell wall thickness could have been capable of producing according to equations 6–9 with the cell wall porosity at a constant value of 0.05, as we initially treated it (Fig. 4a, 4b). This steeper response probably reflects a variation in a model variable that has considerable influence on r_m, and that was taken as a constant in the initial analyses. Consider first the possibility that such a variable occurred in equations 6–9 and was measured for different species. For example, cell wall thickness might have been correlated with low S_c/S increasing mesophyll resistance by narrowing the pathway into cells or with a low fraction of intercellular airspace increasing gas-phase resistance. But, in both cases, the variable would have influenced the estimate of mesophyll resistance made from anatomical measurements through equations 6–9, and that estimate would have been correlated with mesophyll cell wall thickness in the same manner as the mesophyll resistance measured through gas exchange, shown in Fig. 4a. However, the mesophyll resistance calculated from anatomy (Fig. 4b) was much more weakly correlated with cell wall thickness, the relationship being only about as strong as expected from the direct influence of cell wall thickness on resistance.

It follows, therefore, that the extra variable correlated with cell wall thickness and it was not treated as a variable in the calculation by equations 6–9. The likeliest candidate is the porosity of the walls of mesophyll cells. Initially this was treated as a constant of 0.05 in the calculations described above, which resulted in reasonable total mesophyll resistance values across species. However, if wall porosity varied substantially and was correlated with wall thickness, this could account for the stronger effect of cell walls on liquid phase resistance (Fig. 4a, 4b). The resistance imposed by cell walls depends on cell wall porosity, the tortuosity of pores, and cell wall thickness. Values for cell wall porosity and tortuosity of the pores are poorly known (Evans *et al.*, 2009); for example, porosities suggested in the literature include 0.05, 0.07, 0.1 or 0.3 (Evans *et al.*, 2009; Nobel, 1991; Terashima *et al.*, 2006). It was noted by Terashima *et al.* (2006) that cell wall porosity might vary considerably across species, and that r_{cw} would become an important factor determining internal diffusion resistance at porosities below 0.1. When porosity was modelled as varying from 0.040 to 0.095 and as being negatively correlated with cell wall thickness, then cell wall thickness contributed to variation in r'_m as much as that observed (Fig. 4). The effect of assuming porosity varying in conjunction with cell wall thickness was to make wall resistance at least as important as S_c/S as a source of variation across species in determining mesophyll resistance (Figs. 3,4).

It is emphasized that the linear decline of mesophyll cell wall porosity with cell wall thickness used in our calculations is hypothetical and should not be interpreted as a measured relationship. There are no direct measurements of cell wall porosity, and it remains logically possible that the discrepancy between Fig. 4a and 4b could be resolved by a correlation between cell wall thickness and some other trait that increased resistance. Nevertheless, our provisional opinion is that the most biologically plausible explanation is for thicker cell walls to be more lignified and have less pore volume per unit depth.

Structural limitations to photosynthesis measured in the field

According to our model calculations, and to our results (Fig. 6a, 6b), there are two main sources of variation in r_m across Australian sclerophyll species: t_{cw} and S_c/S.

Previously, a strong negative relationship between r_m and S_c/S in annual species with thin cell walls has been demonstrated by Evans *et al.* (1994), whereas the correlation was far weaker

among forest tree species with thicker mesophyll cell walls (Terashima *et al*., 2006), as also seen here. No effect of S_c/S on r_m was shown by Kogami *et al*. (2001). The cause of such a difference between studies is probably higher t_{cw} in evergreen and some deciduous species (Terashima *et al*., 2006). Here, HRLN and LRHN species had significantly thicker cell walls (Table 3) and, consequently, had generally higher r_m per $(S_c/S)^{-1}$ (Fig. 4). This suggests that the negative effect of a longer diffusion pathway dominates over the positive effect of high S_c/S in species with thicker mesophyll cell walls.

Since r_m varies widely across Australian sclerophyll species and it is higher in leaves with thicker cell walls, the question arises to what extent photosynthesis is limited by r_m. It has been suggested that the degree to which photosynthesis is limited by structure is approximately invariant across species (Evans and Loreto, 2002). However, a number of subsequent studies have demonstrated that C_i–C_c does, in fact, vary among species (Warren, 2008); for example, it is generally higher in high LMA leaves with robust structure (Niinemets *et al*., 2005; Niinemets and Sack, 2006), and in leaves with thicker cell walls (current study). By contrast, C_c varied little among the five *Banksia* species studied by Hassiotou *et al*. (2009). Yet, just as here, there was a strong negative relationship between g_m (r_m=1/g_m) and t_{cw}. Overall, these results collectively suggest that in Australian sclerophyll species photosynthesis is more limited by r_m in leaves with thicker cell walls.

Integrative trait LMA fails to predict r$_m$ across broad sample of species

Flexas *et al*. (2008) drew an upper boundary of r_m versus LMA relationship that increased linearly with increasing LMA. The trend, when extrapolated, predicts an infinite r_m at an LMA of about 250 g m^{-2}. However, in Australian sclerophylls, r_m and C_i–C_c were in the same range as those in other broad-leaved evergreen sclerophyll species, although Australian sclerophyll leaves possess somewhat greater LMA values (Niinemets *et al*., 2009*b*; Hassiotou *et al*., 2010).

According to Syvertsen *et al*. (1995); Hanba *et al*. (1999, 2001), Miyazawa and Terashima (2001); Terashima *et al*. (2001, 2006), and Tosens *et al*. (2012), t_{cw} varies from 0.2–0.3 μm in deciduous species and from 0.3–0.5 μm in evergreen species, whereas S_c/S varies from 8–23 m^2 m^{-2}. Anatomical measurements from this study indicate that, in these highly sclerophyllous species S_c/S and t_{cw} are in the same range as reported for other sclerophylls and deciduous tree species (accordingly, 8–22 m^2 m^{-2} and 0.252–0.420 μm, see also Tables 2 and 4). Similarly, Hassiotou *et al*. (2010) reported t_{cw} values from approximately 0.23–0.43 μm in *Banksia* species. Although r_m often correlates with the integrative trait LMA (Niinemets *et al*., 2009*c*), Australian species are outliers in the general LMA and r_m relationship (Hassiotou *et al*., 2009; Niinemets *et al*., 2009*b*). While, in other sclerophylls, thick-walled mesophyll is distributed uniformly between the epidermal layers, in Australian sclerophylls (e.g. Proteaceae) there is characteristically a heterogeneous distribution of thick-walled sclerenchyma and mesophyll islands, where the individual mesophyll cell does not necessarily have thick cell walls (Jordan *et al*., 2005; Niinemets *et al*., 2009*b*).

How Australian sclerophyll leaves increase S$_c$/S

According to the model predictions, one of the most important sources of variation in r_m was S_c/S. That led us to the question of what features of leaves are conducive to exposing large areas of chloroplast at the cell surfaces per unit surface area of the leaf. It is commonly assumed that increased t_{leaf} reflects both higher S_c/S as well as S_{mes}/S (Hanba *et al*., 2002, Terashima *et al*., 2006), and across annuals and deciduous species this relationship does indeed seem to hold (Evans *et al*., 1994; Hanba *et al*., 1999; Terashima *et al*., 2006; Tosens *et al*., 2012). However, across the woody sclerophyll species studied in this work, S_c/S did not correlate with leaf (or mesophyll) thickness (see Supplementary Fig. S1a, b at *JXB* online). Similarly, Slaton and Smith (2002) analysed species across a wide range of genera and did not find a positive correlation between S_{mes}/S and t_{mes}.

Thick leaves have been considered disadvantageous because of increased gas phase resistance (Parkhurst, 1994; Terashima *et al*., 2001). In the leaves of *Hakea dactyloides* (Proteaceae) the thickest in this study, r_{gas} contributed 30% of r_m. Presumably thick-leaved sclerophyll species would most benefit from minimizing gas phase resistance as much as possible and organizing their mesophyll to that end. For example, S_c/S can be increased (Terashima *et al*., 2011) by having several layers of small palisade cells (Figs 8a, 8d), by having armed type cells (Fig. 8b, shown within the circle (as noted by Terashima *et al*., 2011, armed cells having lobes help to increase S_c/S) or by cell elongation (Fig. 8c). The palisade cells were small in most of the species studied here (Fig. 8a, 8b, 8d). Out of these strategies, only cell elongation might require a simultaneous increase in leaf thickness, but otherwise it is just a matter of mesophyll architecture. By having small-celled leaves can decrease gas phase resistance and simultaneously increase S_c/S (Terashima *et al*., 2006). Hassiotou *et al*. (2010) reported a positive correlation between the length of palisade cells and leaf thickness in *Banksia* species. In our study the fraction of mesophyll composed of palisade varied from 50–90% (see Supplementary Table S1 at *JXB* online). This fraction was positively correlated with S_c/S (Fig. 7b), indicating that palisade tissue did importantly contribute to S_c/S.

The intercellular airspace volume fraction correlated negatively with S_c/S, indicating that many of the species studied tended to pack their mesophyll tightly and leave just sufficient airspace adjacent to the cell walls for CO_2 dissolution. This contrasts with the positive correlation between the fraction of intercellular air spaces and S_c/S reported for tobacco (Evans *et al*., 1994). As expected, species in our study with high S_{mes}/S also had higher S_c/S (Fig. 7c). This positive relationship has also been reported by Hanba *et al*. (2001) and Terashima *et al*. (2006).

Often it is assumed that higher t_{leaf} reflects higher S_c/S (Hanba *et al*., 1999; Terashima *et al*., 2011). Our data call into question such postulations. Considered across a wide range of species, there was no relationship between S_c/S and leaf (or mesophyll) thickness.

Conclusions

Although advanced three-dimensional models of mesophyll resistance have been developed, parameterizing these models is complicated and laborious for a large number of species,

as studied here. Further, the predictive power of these models has not yet been tested across species. Overall, our calculations demonstrate that r_m can be successfully predicted from a simple 1-dimensional model which assumes that r_m is determined by key structural leaf anatomical traits that determine the diffusion pathway length.

The two strongest sources of variation across species in total mesophyll resistance are the components of liquid phase resistance: S_c/S, the area of chloroplast exposed at the mesophyll cell surfaces per unit surface area of the leaf, and cell wall resistance. These data demonstrate that structural limitations to photosynthesis are more enhanced in leaves with thicker cell walls. As explained above, the steep relationship of liquid phase resistance with cell wall thickness can not be explained by cell wall thickness alone and most likely arises from a further effect of cell wall porosity varying with cell wall thickness. Overall, these data demonstrate that, across the broad sample of species possessing various structural foliage adaptation mechanisms to cope with adverse environmental conditions, simple integrative traits such as LMA alone fail to predict r_m.

Supplementary data

Supplementary data can be found at *JXB* online.

Supplementary Table S1. Contribution (%) of exposed mesophyll surface area per unit of leaf area (S_c/S) that was controlled by palisade mesophyll ($S_{c,pal}/S$) compared with spongy mesophyll ($S_{c,spon}/S$), for the study species from five sites.

Supplementary Fig. S1. Correlations of chloroplast surface area exposed to intercellular airspace per unit leaf area, S_c/S, with (a) leaf thickness, t_{leaf}, and (b) mesophyll thickness, t_{mes}.

Acknowledgements

References

Aalto T, Juurola E. 2002. A three-dimensional model of CO_2 transport in airspaces and mesophyll cells of a silver birch leaf. *Plant, Cell and Environment* **25,** 1399–1409.

Ayub G, Smith RA, Tissue DT, Atkin OK. 2011. Impacts of drought on leaf respiration in darkness and light in *Eucalyptus saligna* exposed to industrial-age atmospheric CO_2 and growth temperature. *New Phytologist* **190,** 1003–1018.

Bernacchi CJ, Singsaas EL, Pimentel C, Portis Jr AR, Long SP. 2001. Improved temperature response functions for models of Rubisco-limited photosynthesis. *Plant, Cell and Environment* **24,** 253–259.

Boron WF, Endeward V, Gros G, Musa-Aziz R, Pohl P. 2011. Intrinsic CO_2 permeability of cell membranes and potential biological relevance of CO_2 channels. *ChemPhysChem* **12,** 1017–1019.

Dodds WS, Stutzman LF, Sollami BJ. 1956. Carbon dioxide solubility in water. *Industrial and Engineering Chemistry. Chemical and Engineering Chemistry Data Series* **1,** 92–95.

Evans JR, Genty B, Kaldenhoff R, Terashima I. 2009. Resistances along the CO_2 diffusion pathway inside leaves. *Journal of Experimental Botany* **60,** 2235–2248.

Evans JR, Loreto F. 2002. Acquisition and diffusion of CO_2 in higher plant leaves. In: Legood RC, Sharkey TD, von Caemmerer S, eds. *Photosynthesis physiology and metabolism*. Dordrecht: Kluwer Academic Publishers, 321–351.

Evans JR, von Caemmerer S, Setchell BA, Hudson GS. 1994. The relationship between CO_2 transfer conductance and leaf anatomy in transgenic tobacco with a reduced content of Rubisco. *Australian Journal of Plant Physiology* **21,** 475–495.

Flexas J, Barbour MM, Cabrera HM, et al. 2012. Mesophyll diffusion conductance to CO_2: an unappreciated central player in photosynthesis. *Plant Science* (in press).

Flexas J, Bota J, Galmes J, Medrano H, Ribas-Carbo M. 2006a. Keeping a positive carbon balance under adverse conditions: responses of photosynthesis and respiration to water stress. *Physiologia Plantarum* **127,** 343–352.

Flexas J, Diaz-Espejo A, Galmés J, Kaldenhoff R, Medrano H, Ribas-Carbó M. 2007. Rapid variations of mesophyll conductance in response to changes in CO_2 concentration around leaves. *Plant, Cell and Environment* **30,** 1284–1298.

Flexas J, Loreto F, Niinemets Ü, Sharkey T. 2009. Special Issue: mesophyll conductance to CO_2: mechanisms, modelling, and ecological implications, Preface. *Journal of Experimental Botany* **60,** 2215–2216.

Flexas J, Ribas-Carbo M, Diaz-Espejo A, Galmes J, Medrano H. 2008. Mesophyll conductance to CO_2: current knowledge and future prospects. *Plant, Cell and Environment* **31,** 602–621.

Flexas J, Ribas-Carbo M, Hanson DT, Bota J, Otto B, Cifre J, McDowell N, Medrano H, Kaldenhoff R. 2006b. Tobacco aquaporin NtAQP1 is involved in mesophyll conductance to CO_2 *in vivo*. *The Plant Journal* **48,** 427–439.

Gillon JS, **Yakir D.** 2000. Internal conductance to CO_2 diffusion and $C^{18}OO$ discrimination in C_3 leaves. *Plant Physiology* **123,** 201–214.

Gorton HL, Herbert SK, Vogelmann TC. 2003. Photoacustic analysis indicates that chloroplast movement does not alter liquid-phase CO_2 diffusion in leaves of *Alocasia brisbanensis*. *Plant Physiology* **132,** 1529–1539.

Groom PK, Lamont BB, Markey AS. 1997. Influence of leaf type and plant age on leaf structure and sclerophylly in *Hakea* (Proteaceae). *Australian Journal of Botany* **45,** 827–838.

Hanba YT, Kogami H, Terashima I. 2002. The effect of growth irradiance on leaf anatomy and photosynthesis in *Acer* species differing in light demand. *Plant, Cell and Environment* **25,** 1021–1030.

Hanba YT, Miyazawa SI, Kogami H, Terashima I. 2001. Effects of leaf age on internal CO2 transfer conductance and photosynthesis in tree species having different types of shoot phenology. *Australian Journal of Plant Physiology* **28,** 1075–1084.

Hanba YT, Miyazawa SI, Terashima I. 1999. The influence of leaf thickness on the CO_2 transfer conductance and leaf stable carbon isotope ratio for some evergreen tree species in Japanese warm-temperate forests. *Functional Ecology* **13,** 632–639.

Hanba YT, Shibasaka M, Hayashi Y, Hayakawa T, Kasamo K, Terashima I, Katsuhara M. 2004. Overexpression of the barley aquaporin HvPIP2;1 increases internal CO_2 conductance and CO_2 assimilation in the leaves of transgenic rice plants. *Plant and Cell Physiology* **45,** 521–529.

Harley PC, Loreto F, di Marco G, Sharkey TD. 1992. Theoretical considerations when estimating the mesophyll conductance to CO_2 flux by analysis of the response of photosynthesis to CO_2. *Plant Physiology* **98,** 1429–1436.

Hassiotou F, Ludwig M, Renton M, Veneklaas EJ, Evans JR. 2009. Influence of leaf dry mass per area, CO_2, and irradiance on mesophyll conductance in sclerophylls. *Journal of Experimental Botany* **60,** 2303–2314.

Hassiotou F, Renton M, Ludwig M, Evans JR, Veneklaas EJ. 2010. Photosynthesis at an extreme end of the leaf trait spectrum: how does it relate to high leaf dry mass per area and associated structural parameters? *Journal of Experimental Botany* **61,** 3015–3028.

Jordan GJ, Dillon RA, Weston PH. 2005. Solar radiation as a factor in evolution scleromorphic leaf anatomy in Proteaceae. *American Journal of Botany* **92,** 789–796.

Kogami H, Hanba YT, Kibe T, Terashima I, Masuzawa T. 2001. CO2 transfer conductance, leaf structure and carbon isotope composition of *Polygonum cuspidatum* leaves from low and high altitudes. *Plant, Cell and Environment* **24,** 529–538.

Loreto F, Harley PC, di Marco G, Sharkey TD. 1992. Estimation of mesophyll conductance to CO_2 flux by three different methods. *Plant Physiology* **98,** 1437–1443.

Missner A, Kügler P, Saparov SM, Sommer K, Mathai JC, Zeidel ML, Pohl P. 2008. Carbon dioxide transport through membranes. *Journal of Biological Chemistry* **283,** 25340–25347.

Miyazawa SI, Terashima I. 2001. Slow development of leaf photosynthesis in an evergreen broad-leaved tree, *Castanopsis sieboldii*: relationships between leaf anatomical characteristics and photosynthetic rate. *Plant, Cell and Environment* **24,** 279–291.

Mullin LP, Sillett SC, Koch GW, Tu KP, Antoine ME. 2009. Physiological consequences of height-related morphological variation in *Sequoia sempervirens* foliage. *Tree Physiology* **29,** 999–1010.

Niinemets Ü, Cescatti A, Rodeghiero M, Tosens T. 2005. Leaf internal diffusion conductance limits photosynthesis more strongly in older leaves of Mediterranean evergreen broad-leaved species. *Plant, Cell and Environment* **28,** 1552–1566.

Niinemets Ü, Diaz-Espejo A, Flexas J, Galmes J, Warren CR. 2009a. Importance of mesophyll diffusion conductance in estimation of plant photosynthesis in the field. *Journal of Experimental Botany* **60,** 2271–2282.

Niinemets Ü, Díaz-Espejo A, Flexas J, Galmés J, Warren CR. 2009c. Role of mesophyll diffusion conductance in constraining potential photosynthetic productivity in the field. *Journal of Experimental Botany* **60,** 2249–2270.

Niinemets Ü, Flexas J, Peñuelas J. 2011. Evergreens favored by higher responsiveness to increased CO_2. *Trends in Ecology and Evolution* **26,** 136–142.

Niinemets Ü, Reichstein M. 2003a. Controls on the emission of plant volatiles through stomata: differential sensitivity of emission rates to stomatal closure explained. *Journal of Geophysical Research* **108,** 4208, doi:10.1029/2002JD002620.

Niinemets Ü, Reichstein M. 2003b. Controls on the emission of plant volatiles through stomata: a sensitivity analysis. *Journal of Geophysical Research-Atmospheres* **108,** 4211, doi:4210.1029/2002JD002626.

Niinemets Ü, Sack L. 2006. Structural determinants of leaf light-harvesting capacity and photosynthetic potentials. *Progress in Botany* **67,** 385–419.

Niinemets Ü, Wright IJ, Evans JR. 2009b. Leaf mesophyll diffusion conductance in 35 Australian sclerophylls covering a broad range of foliage structural and physiological variation. *Journal of Experimental Botany* **60,** 2433–2449.

Nobel PS. 1991. *Physiochemical and environmental plant physiology*, 4th edn. San Diego, California: Academic Press,.

Parkhurst DF. 1994. Tansley review no. 65. Diffusion of CO_2 and other gases inside leaves. *The New Phytologist* **126,** 449–479.

Piel C, Frak E, Le Roux X, Genty B. 2002. Effect of local irradiance on CO_2 transfer conductance of mesophyll in walnut. *Journal of Experimental Botany* **53,** 2423–2430.

Pons TL, Flexas J, von Caemmerer S, Evans JR, Genty B, Ribas-Carbo M, Brugnoli E. 2009. Estimating mesophyll conductance to CO_2: methodology, potential errors, and recommendations. *Journal of Experimental Botany* **60,** 2217–2234.

Price D, von Caemmerer S, Evans JR, Yu JW, Lloyd J, Oja V, Kell P, Harrison K, Gallagher A, Badger M. 1994. Specific reduction of chloroplast carbonic anhydrase activity by antisense. RNA in transgenic tobacco plants has a minor effect on photosynthetic CO_2 assimilation. *Planta* **193,** 193–331.

Rodeghiero M, Niinemets Ü, Cescatti A. 2007. Major diffusion leaks of clamp-on leaf cuvettes still unaccounted: how erroneous are the estimates of Farquhar et al. model parameters? *Plant, Cell and Environment* **30,** 1006–1022.

Slaton MR, Smith WK. 2002. Mesophyll architecture and cell exposure to intercellular air space in alpine, desert, and forest species. *International Journal of Plant Sciences* **163,** 937–948.

Steppe K, Niinemets Ü, Teskey R.O. 2011. Tree size- and age-related changes in leaf physiology and their influence on carbon gain. In: Meinzer FC, Dawson T, Lachenbruch B, eds. *Size- and age-related changes in tree structure and function*. Berlin: Springer, 235–253.

Syvertsen JP, Lloyd J, McConchie C, Kriedemann PE, Farquhar GD. 1995. On the relationship between leaf anatomy and CO_2 diffusion through the mesophyll of hypostomatous leaves. *Plant, Cell and Environment* **18,** 149–157.

Terashima I, Hanba YT, Tazoe Y, Vyas P, Yano S. 2006. Irradiance and phenotype: comparative eco-development of sun and shade leaves in relation to photosynthetic CO_2 diffusion. *Journal of Experimental Botany* **57,** 343–354.

Terashima I, Hanba YT, Tholen D, Niinemets Ü. 2011. Leaf functional anatomy in relation to photosynthesis. *Plant Physiology* **155,** 108–116.

Terashima I, Ishibashi M, Ono K, Hikosaka K. 1995. Three resistances to CO_2 diffusion: leaf-surface water, intercellular spaces and mesophyll cells. In: Mathis P, ed. *Photosynthesis: from light to biosphere*, Vol. V. Dordrecht: Kluwer Academic Publishers, 537–542.

Terashima I, Miyazawa SI, Hanba YT. 2001. Why are sun leaves thicker than shade leaves? Consideration based on analyses of CO_2 diffusion in the leaf. *Journal of Plant Research* **114,** 93–105.

Tholen D, Zhu X-G. 2011. The mechanistic basis of internal conductance: a theoretical analysis of mesophyll cell photosynthesis and CO_2 diffusion. *Plant Physiology* **156,** 90–105.

Tosens T, Niinemets Ü, Vislap V, Eichelmann H, Castro-Díez P. 2012. Developmental changes in mesophyll diffusion conductance and photosynthetic capacity under different light and water availabilities in *Populus tremula*: how structure constrains function. *Plant, Cell and Environment* **35,** 839–856.

Ullmann I. 1989. Stomatal conductance and transpiration of *Acacia* under field conditions: similarities and differences between leaves and phyllodes. *Trees: Structure and Function* **3,** 45–56.

Umbreit WW, Burris RH, Stauffer JF. 1972. *Manometric and biochemical techniques. A manual describing methods applicable to the study of tissue metabolism*, 5th edn. Minneapolis: Burgess Publishing Company.

Warren CR. 2008. Stand aside stomata, another actor deserves centre stage: the forgotten role of the internal conductance to CO_2 transfer. *Journal of Experimental Botany* **59,** 1475–1487.

Warren CR, Adams M. 2006. Internal conductance does not scale with photosynthetic capacity: implications for carbon isotope discrimination and the economics of water and nitrogen use in photosynthesis. *Plant, Cell and Environment* **29,** 192–201.

Weisiger R. 1998. Impact of extracellular and intracellular diffusion barriers on transport. In: Bassingthwaighte JB, Goresky CA, Linehan JH, eds. *Whole organ approach to cellular metabolism*. New York: Springer-Verlag, 389–423.

Williams TG, Flanagan LB, Coleman JR. 1996. Photosynthetic gas exchange and discrimination against $^{13}CO_2$ and $C^{18}O^{16}O$ in tobacco plants modified by an antisense construct to have low chloroplastic carbonic anhydrase. *Plant Physiology* **112,** 319–326.